Vol. 66, No. 10

Cloning and Molecular Characterization of a cDNA Clone Coding for *Trichomonas vaginalis* Alpha-Actinin and Intracellular Localization of the Protein

MARIA FILIPPA ADDIS, PAOLA RAPPELLI, GIUSEPPE DELOGU, FRANCO CARTA,
PIERO CAPPUCCINELLI, AND PIER LUIGI FIORI*

*Division of Experimental and Clinical Microbiology, Department of Biomedical Sciences,
University of Sassari, Sassari, Italy*

We have identified and sequenced a cDNA clone coding for *Trichomonas vaginalis* alpha-actinin. Analysis of the obtained sequence revealed that the 2,857-nucleotide-long cDNA contained an open reading frame encoding 849 amino acids which showed consistent homology with alpha-actinins of different species. Such homology was particularly significant in regions which have been reported to represent the actin-binding and Ca^{2+}-binding domains in other alpha-actinins. The deduced protein was also characterized by the presence of a divergent central region thought to play a role in its high immunogenicity. A study of protein localization performed by immunofluorescence revealed that the protein is diffusely distributed throughout the *T. vaginalis* cytoplasm when the cell is pear shaped. When parasites adhere and transform into the amoeboid morphology, the protein is located only in areas close to the cytoplasmic membrane and colocalizes with actin. Concomitantly with transformation into the amoeboid morphology, alpha-actinin mRNA expression is upregulated.

The flagellated protozoan parasite *Trichomonas vaginalis* is the etiologic agent of one of the most widespread sexually transmitted diseases worldwide. The main pathological manifestations of a trichomonad infection in women are abdominal pain, itching, and presence of a foul-smelling discharge with abundant leukocytes (19), while in men the infection is mostly asymptomatic, although it can sometimes lead to urethritis, prostatitis, and epididymitis (24). The infection recently has been associated with severe complications, such as infertility (28), enhanced predisposition to neoplastic transformation in cervical tissues (37), and progression of human immunodeficiency virus (27, 35).

Pathogenesis occurs via cytopathogenicity against vaginal epithelial cells (18). Several in vitro studies have reported that adhesion of the parasite to the target cell is essential for the maintenance of infection and for cytopathogenicity (2, 25). Using erythrocytes as a target cell model, we recently demonstrated that the cytopathic effect of *T. vaginalis* is mediated by pH-dependent perforins (1, 14) and by a contact-dependent disruption of the cortical cytoskeleton (13). The results obtained in our studies highlighted the importance of an intimate association between the parasite and the target cell membranes. Contact of *T. vaginalis* with epithelial cells induces significant changes in parasite morphology. The ability of *T. vaginalis* to change from ellipsoidal to amoeboid morphology when it encounters the target cell seems to represent a virulence trait (5). Moreover, the motility and plasticity of the parasite are important for pathogenic activity (16). The ability to undergo a morphological transformation upon contact with the target cell requires the presence of a complex and ductile cytoskeletal structure, which needs to be finely tuned and able to respond promptly to external stimuli. The parasite cytoskeleton has been the subject of different studies (7, 22), but the

relationships between the molecular components of this structure and the morphological changes that occur during parasitism have never been studied. It was recently discovered that *T. vaginalis* and other protozoan parasites possess complicated pathways and complex regulation mechanisms which were believed to exist only in higher eukaryotes. For example, the presence in *T. vaginalis* of calmodulin and of E2 ubiquitin-conjugating enzyme was recently reported (23).

During infection, host-parasite interactions are regulated by a cascade of events involving complex intracellular pathways for the signalling and regulation of the expression of virulence genes (5). A detailed study of the parasite cytoskeleton at a molecular level is therefore fundamental for understanding the multiple responses to signals that follow the initial contact event.

In this study, we report the isolation, nucleotide sequencing, and characterization of a cDNA coding for *T. vaginalis* alpha-actinin. Alpha-actinin is an actin-binding, Ca^{2+}-regulated protein involved in actin cross-linking. It is widely distributed among different cellular types. The actin-binding protein family plays a fundamental role in motion and morphological changes, since motion is a consequence of the cellular redistribution of actin.

The alpha-actinin cDNA sequence was characterized at the nucleotide and amino acid levels, revealing several interesting features of the molecule. In addition, a study of the cytoplasmic localization in pear-shaped and amoebic parasites was performed.

MATERIALS AND METHODS

Strains and culture conditions. Thirty *T. vaginalis* isolates were obtained from vaginal specimens of women affected by trichomoniasis in Italy and Mozambique. Organisms were axenically grown in Diamond's Trypticase-yeast medium (10). For experiments in which a single strain was used, we chose isolate SS-22, already used in all our previous works as a standard *T. vaginalis* strain.

Giardia lamblia was kindly provided by L. Gradoni, Istituto Superiore di Sanità, Rome, Italy; *Acanthamoeba castellanii* was a gift from P. Varaldo, University of Ancona, Ancona, Italy; and *Leishmania major* was kindly provided by C. Bordier, University of Lausanne, Lausanne, Switzerland. *Entamoeba histolytica* HK-9 was obtained from the American Type Culture Collection. Protozoa

---

* Corresponding author. Mailing address: Department of Biomedical Sciences, Division of Experimental and Clinical Microbiology, University of Sassari, Viale S. Pietro 43/B, 07100 Sassari, Italy. Phone: 39 79 228301. Fax: 39 79 212345. E-mail: micropat@ssmain.uniss.it.

were cultured either in media suggested by the American Type Culture Collection or by standard procedures (11, 36). *L. major* and HeLa cells were cultured in RPMI medium supplemented with 10% fetal bovine serum, 100 U of penicillin G per ml, and 100 mg of streptomycin per liter at 37°C in a 5% carbon dioxide atmosphere.

The bacterial strain used for recombinant DNA procedures was *Escherichia coli* XL1-Blue grown in Luria-Bertani medium at 37°C in the presence of 100 mg of ampicillin per μl.

Screening of the cDNA library and production of recombinant protein. *T. vaginalis* proteins bound to the target cell surface were detected as described previously (15). Briefly, parasite sonicates obtained in phosphate-buffered saline (PBS) were incubated with erythrocytes. After 2 h of incubation at 37°C, erythrocyte membranes were collected, resuspended in lysis buffer (26), and boiled. Samples were subjected to sodium dodecyl sulfate-polyacrylamide gel electrophoresis in a 7.5% polyacrylamide gel and transferred to nitrocellulose. The portion of the nitrocellulose membrane corresponding to proteins of 110 to 125 kDa was cut, saturated with blocking solution (PBS, 0.05% Tween 20, 5% nonfat milk) for 1 h, and incubated for 2 h with rabbit hyperimmune serum against *T. vaginalis*. After five washes, antibodies bound to the membrane were eluted as described elsewhere (31). The specific activity of the eluted antibodies against a 115-kDa trichomonad protein was confirmed by immunoblotting with a total protein extract of the parasite. The absence of cross-reactivity with erythrocyte proteins was also confirmed by immunoblotting.

The eluted antibodies were used to screen a previously obtained λZAPII cDNA library (31) for recombinant plaques containing the cDNA coding for the 115-kDa protein. Fusion proteins were induced with isopropyl-β-D-thiogalactopyranoside (IPTG), and recombinant plaques were detected with the antibodies eluted as described above. After cloning and purification of reactive plaques, the corresponding pBluescript plasmids were excised. The recombinant plasmids were transformed into *E. coli* XL1-Blue.

Large-scale preparation of monospecific anti–alpha-actinin antibodies was performed. The purified phage clone plaques were induced with IPTG, and the proteins were transferred to nitrocellulose filters. The filters were blocked and incubated with rabbit hyperimmune anti-*T. vaginalis* serum preabsorbed with *E. coli* proteins. Antibodies bound to the recombinant 115-kDa protein were eluted as described before (31).

DNA sequencing and analysis. Sequencing of the 2,851-bp cDNA cloned in pBluescript SK(+) or SK(−) (Stratagene, La Jolla, Calif.) in both senses was performed by the Sanger dideoxy chain termination method with a Sequenase version 2.0 kit (United States Biochemical Corp., Cleveland, Ohio). T3 and T7 primers, recognizing specific regions in the multiple cloning sites, were used initially. As more data about the sequence were obtained, 18- to 20-mer synthetic oligonucleotides were designed and used for the subsequent reaction. Primers were synthesized by use of a Gene Assembler Plus (Pharmacia, Uppsala, Sweden). Computer analysis of the sequence was done with PC/GENE (IntelliGenetics, Inc., Mountain View, Calif.), FASTA (30), and BLAST 2.0.1 (3).

DNA extraction and PCR. Total DNA was extracted from all 30 *T. vaginalis* isolates as described elsewhere (31). One microliter of DNA from each trichomonad strain was submitted to PCR to assess the presence of the alpha-actinin gene. Primers TV44 (5′-TCGCTTCCGTTATCT-3′) and TV45 (5′-AGGAGGTGCTTGATGT-3′), specific for a 513-bp portion of the cDNA, were selected. The final amplification volume of 25 μl contained 10 mM Tris HCl (pH 8.80), 50 mM KCl, 1.5 mM MgCl$_2$, 0.1% Triton X-100, 200 μM each deoxynucleotide triphosphate, 12.5 pmol of each primer, and 0.5 U of DynaZyme thermostable DNA polymerase (Fynnzymes, Oy, Finland). Amplification was performed with a Hybaid thermal cycler (35 cycles consisting of denaturation at 94°C for 45 s, annealing at 48°C for 45 s, and extension at 72°C for 1 min). Amplification products were electrophoresed in a 1% agarose gel and visualized with a UV transilluminator after ethidium bromide staining.

RNA extraction, Northern blot analysis, and reverse transcription (RT)-PCR. Total trichomonad RNA extraction was performed with *T. vaginalis* SS-22 as described by Chomczynski and Sacchi (9). *T. vaginalis* cells grown in plastic flasks were separated into two populations: pear-shaped parasites in suspension and amoebic parasites adhering to the flasks. Pear-shaped parasites were collected from the supernatant, washed three times with PBS, and treated for RNA extraction. The flasks with the adhering parasites were washed three times with PBS, and adhering *T. vaginalis* organisms were treated for RNA extraction. The RNA obtained was quantified, tested for quality and purity, and stored at −70°C until further use.

The extracted, quantified RNA was electrophoresed in 1% agarose–2 M formaldehyde gels (32) and transferred to Hybond-N membranes (Amersham). The DNA probe used to detect alpha-actinin mRNA was prepared by PCR with primers TV44 and TV45, while the DNA probe used to detect actin mRNAs was obtained with primers Tvact1 (TGTCGGCCGTCCAAAGTA) and Tvact2 (ATCACGGCCAGCGAGGTTA) (7) by the procedure described above but with the inclusion of a digoxigenin-labeled deoxynucleotide in the reaction mixture (Boehringer Mannheim Biochemicals). Prehybridization and hybridization were performed overnight by standard procedures (32). Hybridized filters were extensively washed and incubated for 1 h with alkaline phosphatase-conjugated anti-digoxigenin antibody (Boehringer). The filters were washed again, and the reaction was revealed according to the manufacturer's suggestions.

For RT-PCR, RNA samples were pretreated with DNase, and 1.2 μg was

incubated at 65°C for 10 min after the addition of 0.1 μg of oligo(dT). After incubation, 4 μl of 5× reaction buffer, 2 μl of each deoxynucleotide triphosphate at 1.25 mM, 2 μl of 0.1 M dithiothreitol, and 200 U of Moloney murine leukemia virus reverse transcriptase (Gibco BRL) were added in ice, and the mixture was incubated at 37°C for 1 h and then at 94°C for 5 min. The obtained cDNA was used as a template for PCR under the same conditions as those described above.

Western blot analysis. HeLa cells, parasites, and recombinant *E. coli* were washed three times in PBS. Washed cells were resuspended in lysis buffer (26) without bromphenol blue and boiled for 3 min. Samples were evaluated for protein concentration by the Bradford method (6) with Bio-Rad protein assay dye (Coomassie brilliant blue) and bovine serum albumin as a standard. After protein quantification, bromphenol blue was added, and the same protein amount per sample was loaded on a 7.5% polyacrylamide gel. After the electrophoretic run, the gel was stained with Coomassie brilliant blue. A replica of the gel was Western blotted onto nitrocellulose, blocked with blocking solution, and incubated with the eluted anti–*T. vaginalis* alpha-actinin antibodies. The reaction was revealed with alkaline phosphatase-conjugated antibodies and chromogenic substrates.

Indirect immunofluorescence. *T. vaginalis* SS-22 organisms were grown in suspension or seeded on round 12-mm coverslips in 24-well flat-bottom tissue culture plates containing Diamond's Trypticase-yeast medium plus 10% serum. *T. vaginalis* cells seeded on coverslips were allowed to adhere and transform into the amoeboid form. Samples were washed with PBS, fixed with 3.7% paraformaldehyde for 1 h, treated with 0.25% Triton X-100 for 30 s, and incubated for 1 h with PBS containing 3% bovine serum albumin. For visualization of alpha-actinin, samples were incubated with rabbit anti–*T. vaginalis* alpha-actinin antibodies for 1 h, with PBS–1% bovine serum albumin for 30 min, and then with fluorescein isothiocyanate-labeled goat anti-rabbit antibodies preabsorbed with parasites for 30 min.

Colocalization experiments were performed with *T. vaginalis* organisms fixed on coverslips as described above. Coverslips were coincubated with rabbit anti–*T. vaginalis* alpha-actinin antibodies and antiactin monoclonal antibodies (clone AC-40; Sigma Chemical Co., St. Louis, Mo.). *T. vaginalis* alpha-actinin was visualized with fluorescein isothiocyanate-labeled goat anti-rabbit antibodies, while actin was visualized with tetramethyl rhodamine isothiocyanate-labeled goat anti-mouse immunoglobulin G antibodies. Samples were observed with an epifluorescence microscope. The anti–alpha-actinin antibodies used in these assays were obtained by elution from the screened, purified recombinant phage plaques expressing recombinant *T. vaginalis* alpha-actinin. Preimmune serum and secondary antibodies did not produce any fluorescence of trichomonad cells.

In order to further confirm the absence of cross-reactivity between parasite and human alpha-actinin, *T. vaginalis* SS-22 cells were incubated with a semiconfluent HeLa cell monolayer grown in RPMI medium plus serum on coverslips. The incubation mixture was monitored for the absence of target cell lysis in order to avoid the presence of the parasite adhesive proteins on the surface of lysed cells (15). *T. vaginalis* cells incubated with HeLa cells were allowed to adhere and transform into the amoeboid form. Coverslips were processed as described above.

Nucleotide sequence accession number. The GenBank accession number of the cDNA encoding *T. vaginalis* alpha-actinin is AF014928.

RESULTS

Isolation of cDNA clones and expression of the recombinant gene. Previous studies performed on *T. vaginalis* adhesive proteins led us to the observation that erythrocytes lysed by the microorganism displayed both the major adhesive proteins already described in previous studies (4, 15) and a 115-kDa trichomonad protein that was present in small amounts. The protozoan protein was present on the host cell surface after completion of lysis by live *T. vaginalis* or after incubation of target cells with protozoan lysates. In order to identify and characterize the 115-kDa *T. vaginalis* protein, specific antibodies were eluted from a rabbit hyperimmune anti-*T. vaginalis* serum. The eluted antibodies, which were monospecific and did not show cross-reactivity with target cell proteins, were used to screen a *T. vaginalis* cDNA expression library. The screening led to the isolation of several positive phage clones. One of the clones was chosen, and the pBluescript (SK)− plasmid was excised and used to transform competent *E. coli* cells. The transformed cells produced a recombinant protein of about 110 kDa, suggesting that the cDNA clone coded for almost the entire sequence. The recombinant protein was readily recognized by antibodies eluted from the 115-kDa native protein bound to erythrocytes (data not shown). More-

A

```
1     NSARGREGLL DDAWEKTQIK VFSRWVQKQL LARQIQFETI ETDFEDGTKL

51    LNLLEIIGKE PMPGKWHKQP KMMVQKRETV DIALKYINEV KKIRTVGIGA

101   DDIINKNLKL TLGLTWTCIN KFMIEEISVE EATARDALLL WAKKNTQGYE

151   HVAVNNFTTS WNTGLAFAAL INKFRPNLLD YSALDYNDHK GACEKAFAAC

201   KELGIYVYLD PEDVIDTTPD EKSVVTQVAE FFHFFASESK IAAMADKIKR

251   TVAIQKQIDE LKNTYIEDAK AAIEKMTVED EKLKADDYEK TIPGIRGKLA

301   SVISYNRDIR PEIVDHRAKA MRSWAALVTK CKSGNRPIPE IPQGLEPEAL

351   TNKFNEIEQT STTRRDELTQ ELNDMIKKKV EDFMAKCMDI INKCDAIHEE

401   VKTIEGTTAE KKDKVEOKLH EAEDLQPALA ELTPLFQELV ELRINTLSSQ

451   TDDSVNRHHS QLITYIKHLL EQLNGKLFEE TNEARINEYN ALAQPLYDEA

501   IAFKEEVLAI SGELRERRTQ FLAKQAEAPT KREHVNEIDP IFDGLEKDSL

551   HLRVNHSPTE IRNVYAVTLQ HIITELNKIF EEMVANFDAT AVPIIDGITA

601   LVTSSHQIPG DAAAVKAQVE ENLASLDCVR RKDPSPPGSI QRARSIQAQL

651   IKVTYTYSDA TGELVQARLD LKQIILAKKT FLEEEERKAR INNYTVKADE

701   HMNEAHALDG KINSVDGELE PKRQKLYEVR EEVNAKKEKA VEELTPIYED

751   LEKDQLHLEI TSTPASINIF FENLIAHIDT LVKEIDARIA AAKGLEISEE

801   ELNEFKDTFK YFDKDKSNSL EYFELKACLT ALGEDITDDQ AKEYCKKSL
```

B

Source of sequence	Sequence comparison
Tv alpha-actinin	TVGIGADDII NKNLKLTLGL TWTCINKF
Dd alpha-actinin 3	LVGIGAEELV DKNLKMTLGL IWTIILRF
Human alpha-actinin 3	LVSIGAEEIV DGNLKMTLGN IWTIILRF
Drome alpha-actinin	LVSIGAEEIV DGNLKMTLGN IWTIILRF
Chick alpha-actinin	LVSIGAEEIV DGNVKMTLGN IWTIILRF
Consensus	lV-IGAeeiv d-NlKmTLGm iWTiIlrF

C

Source of sequence	Sequence comparison
Tv alpha-actinin	EFKDTFKYFD KDKSNSLEYF ELKACLTAL
Dd alpha-actinin 3	EFKACFSHFD KDNDNKLNRL EFSSCLKSI
Human alpha-actinin 3	EFRASFNHFD RKRNGMMEPD DFRACLISM
Drome alpha-actinin	EFRSSFNKFD KNRTGRLSPE EFKSCLVSL
Chick alpha-actinin	EFRASFNHFD RDHSGTLGPE EFKACLISL
Consensus	EL--LL--LD -D-D---D-- DL--LL—L
Ca2+ chelating	x y z-y-x -z

FIG. 1. (A) Deduced amino acid sequence of the *T. vaginalis* alpha-actinin cDNA. The actin-binding site and the EF-hand domain are shown in bold. The underlined amino acids represent the central, divergent region. (B) Homology between actin-binding site of *T. vaginalis* alpha-actinin and actin-binding sites of other alpha-actinins. Consensus indicates the most frequent amino acid at that position. Uppercase letters indicate that the amino acid is present in all peptides; lowercase letters indicate the most common amino acid. (C) Homology between EF-hand (Ca²⁺-chelating domain) of *T. vaginalis* alpha-actinin and EF-hands of other alpha-actinins. Consensus indicates the EF-hand consensus sequence (33). The calcium-chelating side chains are also shown (x, y, z-y-x, and -z). D, oxygen-containing side chain; L, hydrophobic side chain; Tv, *T. vaginalis*; Dd, *D. discoideum*; Drome, *D. melanogaster*.

over, antibodies eluted from the recombinant plaques recognized the native protein.

DNA sequencing and characterization. Only one open reading frame was predicted for the cloned cDNA, spanning nucleotides 1 to 2548. The derived amino acid sequence is represented in Fig. 1A. A scan of SWISS-PROT and GenBank revealed significant similarity of the amino acid sequence with alpha-actinins from different species. The amino acid sequence showed 26% identity with *Dictyostelium discoideum* and *Dro-*

sophila melanogaster alpha-actinins (45 and 43%, respectively, when conservative changes were considered).

Identity with alpha-actinin was considerably higher in some areas. For the nucleotide sequence, in the 3′ region identity was as high as 54.15% on 698 nucleotides with human alpha-actinin (3), 55.35% on 598 nucleotides with chick alpha-actinin, and 54.97% on 553 nucleotides with rabbit alpha-actinin. Homology was also found with spectrin, being higher for nucleotides 400 to 700, where the sequence showed 60.5% identity with mouse beta-spectrin. The 5′ region of the sequence displayed very high identity with different calmodulin genes. Nucleotides 2357 to 2522 showed 72 to 64% identity with genes for calmodulins of different species. Consistent with the early divergence of this protozoan parasite, the highest identity was observed with genes for calmodulins of several plants, such as wheat, barley, and maize.

The N-terminal region of the translated sequence was the area where identity with alpha-actinin was higher. In the region spanning amino acids 93 to 197, the sequence was 49% identical to *D. discoideum* alpha-actinin. Identity was increased to 78% when conservative changes were considered. This region contains the domain responsible for the binding of actin in actin-binding proteins. Figure 1B shows the actin-binding domains of other alpha-actinins and a consensus sequence for the actin-binding domain. Moreover, comparison of the *T. vaginalis* alpha-actinin cDNA translated sequence revealed identity with other proteins belonging to the actin-binding protein family, such as spectrin, dystrophin, and myosin. Amino acids from positions 4 to 386, for example, displayed 29% identity (49% similarity) to the *D. melanogaster* spectrin β-chain. Analysis of the protein sequence confirmed the high homology with calmodulin observed in the 5′ region of the nucleotide sequence.

The C-terminal region of the protein (amino acids 803 to 833) contains a Ca²⁺-binding domain known as the EF-hand. Figure 1C shows the alignment of this domain with the EF-hands of other known alpha-actinins and with the consensus sequence given by Tufty and Kretsinger (33) for chick alpha-actinin. The *T. vaginalis* alpha-actinin EF-hand appears to be functional, since it is similar to the consensus sequence. Intracellular rearrangement of the protein could therefore be mediated by signalling mechanisms involving Ca²⁺ ions.

The central region of the protein (amino acids 387 to 650), as shown in Fig. 2, showed less significant homology with alpha-actinin and other cytoskeletal proteins. Analysis of the amino acid sequence for antigenic peptides revealed that some of the predicted areas of highest antigenicity were located in this region (amino acids 682 to 687, 409 to 414, and 377 to 382). The diversity of this region from human alpha-actinin might be interesting in terms of the immunogenicity of the protein.

As expected for a structural protein, the gene coding for the molecule was present in all 30 *T. vaginalis* strains tested, independent of the geographical origins of the patients (data not shown).

Specificity of the *T. vaginalis* alpha-actinin immunogenic determinants. A high degree of identity was observed between the trichomonad alpha-actinin and alpha-actinins from other species. However, the sequence analysis revealed the presence of a divergent peptide region in the central portion of the protein. Computer-assisted analysis revealed that the antigenic determinants most likely were located in this region. Since high identity with other alpha-actinins is present throughout the other regions of the *T. vaginalis* protein, we wanted to test whether antibodies raised against the trichomonad protein reacted with other alpha-actinins of different origins. Since the main targets of *T. vaginalis* in vivo are human epithelial cells, an immunoblot study was performed by probing protein ex-

```
D A I H E E V K T I E G T T A E K K D K V E Q K L H E A E D L Q P A L A E L T P   Tv alpha-actinin.PRO
G L T P N E I D S T W S A L E K A E Q E H A E A L R I E L K R Q K K I A V L L Q   Dd alpha-actinin.PRO
G R M V S D I N N A W G C L E Q V E K G Y E W L L N E I R R L E R L D H L A E     Human alpha-actinin.PRO
G K T V S D I S N S W K G L E L A E K G F E E W L L A E T M R L E R L E H L A Q   Dm alpha-actinin.PRO
G R M V S D I N T G W Q H L E Q A E K G Y E E W L L N E I R R L E P L D H L A E   chick alpha-actinin.PRO

L F Q E L V E L R I N T L S S Q T D D S V N R H H - S Q L I T Y I K H L L E Q     Tv alpha-actinin.PRO
K Y N R I L K K L - E N W A T T K S V Y L G S N E - T G D S I T A V Q A K L K N   Dd alpha-actinin.PRO
K F R Q K A S I H - E A W T D G K E A M L R Q K D Y E T A T L S E I K A L L K K   Human alpha-actinin.PRO
K F K H K A D A H - E D W T R G K E E M L Q S Q D F R Q Y K L N E L K A L K K K   Dm alpha-actinin.PRO
K F R Q K A S I H - E A W T E G K E A M L K Q K D Y E T A T L S D I K A L I R K   chick alpha-actinin.PRO

L N G K L F E - - - - E T N E A R I N E Y N A L A Q P L - - - - Y D E A I A F K   Tv alpha-actinin.PRO
L E A - - F D G E C Q S L E G Q S N S D L L S I L A Q L T E L N Y N G V P E L T   Dd alpha-actinin.PRO
H E A - - F E S D - L A A H Q D R V E Q I A A I A Q E L N E L D Y Y D S P S V N   Human alpha-actinin.PRO
H E A - - F E C D - L A A H Q D R V E Q I A A I A Q E L N T L E Y H D C V C V N   Dm alpha-actinin.PRO
H E A - - F E S D - L A A H Q D R V E Q I A A I A Q E L N E L D Y Y D S P S V N   chick alpha-actinin.PRO

E E V L A I S G E L R E R R T Q F L A K Q A E A P T K R E H - V N E I D P I F D   Tv alpha-actinin.PRO
E R K D T F F A Q Q W T G V K S S A E T Y K N T L L A E L E R L Q K I E D S L V   Dd alpha-actinin.PRO
A R C Q K I - C D Q W D N L G A L T Q K R R E A L E R T E K L L E T I D Q L Y L   Human alpha-actinin.PRO
A R C Q R I - C D Q W D R L G A L T Q R R R T A L D E A E R I L E K I D I L H L   Dm alpha-actinin.PRO
A R C Q K I - C D Q W D V L G S L T H S R R E A L E K T E K Q L E T I D E L H L   chick alpha-actinin.PRO

G L E K - - D S L H L R V N H S P T E I R N V Y A V T L Q H I I T E L N K I F E   Tv alpha-actinin.PRO
E F A K R A A Q L N V W I E A A D D H V - - - F D P I N V D S V Q G V Q E I Q E   Dd alpha-actinin.PRO
E Y A K R A A P F N N W M E G A M E D L Q D T F I V H T I E E I Q G L T T A H E   Human alpha-actinin.PRO
E F A K R A A P F N N W L D G T R E D L V D M F I V H T M V E I Q G L I Q A H D   Dm alpha-actinin.PRO
E Y A K R A A P F N N W M E S A M E D L Q D M F I V H T I E E I E G L I A A H D   chick alpha-actinin.PRO

E M V A N F D A T A - - - - - V P I I D G I T A L V T S S H Q I P G D A A A - -   Tv alpha-actinin.PRO
K F D A F L H D Q S Q Q F A E L E A L A A L T Q Q L R E L - - - - G R S E N D Y   Dd alpha-actinin.PRO
Q F K A T L P D A D K E R L A I L G I H N E V S K I V Q T Y H V N M A G T N P Y   Human alpha-actinin.PRO
Q F K A T L G E A D K E F N L I V N L V R E V E S I V K Q H Q I P G G L E N P Y   Dm alpha-actinin.PRO
Q F K A T L P D A D R E R E A I L G I Q R E A Q R I A D L H S I K L S G N N P Y   chick alpha-actinin.PRO

- - - - - - - - - - - V K A Q V E E N L A S L D C V R R K D P S P P             Tv alpha-actinin.PRO
S V I S Y D E L S A K W N N L L A G I E E R K V Q L A N E L T T Q T N N D         Dd alpha-actinin.PRO
T T I T P Q E I N G K W D H V R Q L V P R R D Q A L T E E H A R Q Q H N E         Human alpha-actinin.PRO
T T L T A N D M T R K W S D V R Q L V P Q R D Q T L A N E R R K Q Q N N E         Dm alpha-actinin.PRO
T S V T P Q V I N S K W E R V Q Q L V P T R D R A L Q D E Q S R Q Q C N E         chick alpha-actinin.PRO
```

FIG. 2. Alignment of the alpha-actinin central region in amino acid sequences from *T. vaginalis* (Tv), *D. discoideum* (Dd), *Homo sapiens* (Human), *D. melanogaster* (Dm), and chick. Boxes represent the amino acids that match those in *T. vaginalis* alpha-actin exactly. The alignment was obtained by the Clustal method with the MegAlign program (Lasergene Suite; DnaStar Inc., Madison, Wis.).

tracts obtained from these cells with anti–trichomonad alpha-actinin antibodies. The results obtained revealed that there was no cross-reactivity; monospecific antibodies directed against *T. vaginalis* alpha-actinin did not recognize the human form of the protein. In order to assess cross-reactivity with other protozoan actin-binding proteins, we tested protein extracts obtained from other protozoan parasites. *G. lamblia*, *E. histolytica*, *A. castellanii*, and *L. major* total proteins were tested. No cross-reactivity was observed with any of them.

The absence of cross-reactivity between parasite and host alpha-actinins was also observed by immunofluorescence. Figure 3 shows the alpha-actinin fluorescence in *T. vaginalis* parasites coincubated with epithelial cells. The localized peripheral fluorescence was clearly visible, while the host cells showed no fluorescence. The lack of fluorescence of epithelial cells confirmed that there was no immunological cross-reactivity between parasite and host proteins, as already shown by the immunoblot studies. Therefore, we hypothesize that anti–trichomonad alpha-actinin antibodies are probably directed against unique antigenic determinants localized in the central, divergent region.

Cellular location of *T. vaginalis* alpha-actinin. Anti–alpha-actinin antibodies were eluted from the purified recombinant plaques incubated with rabbit hyperimmune anti-*T. vaginalis*

serum. Monospecific antibodies were then used to localize alpha-actinin in both pear-shaped and amoeboid, adherent forms of the parasite to investigate its participation in morphological changes. Live *T. vaginalis* cells (>99% viability) grown in suspension and bound on a solid support were fixed and examined by immunofluorescence. Figure 4 shows the immunofluorescence patterns of alpha-actinin in pear-shaped (Fig. 4A) and amoeboid (Fig. 4D) trichomonad cells and in two intermediate stages (Fig. 4B and C). Diffuse, pale fluorescence was observed in the pear-shaped parasites (Fig. 4A), suggesting that intracellular alpha-actinin was located throughout the cytoplasm. When *T. vaginalis* cells bind to a solid support and transform into an amoeboid morphology, an intracellular redistribution of alpha-actinin occurs. As shown in Fig. 4D, the protein fluorescence in amoeboid parasites was observed only in the peripheral, submembranous regions of the trichomonad cell. In intermediate stages, the protein was located at the periphery of the cell (Fig. 4B) and then appeared to be present only in cell protrusions produced during spreading (Fig. 4C). These findings strongly suggest that the protein participates in the formation of pseudopodal extensions and in transformation into the amoeboid morphology.

In order to assess whether the redistribution of *T. vaginalis* alpha-actinin is related to actin redistribution in the same cel-
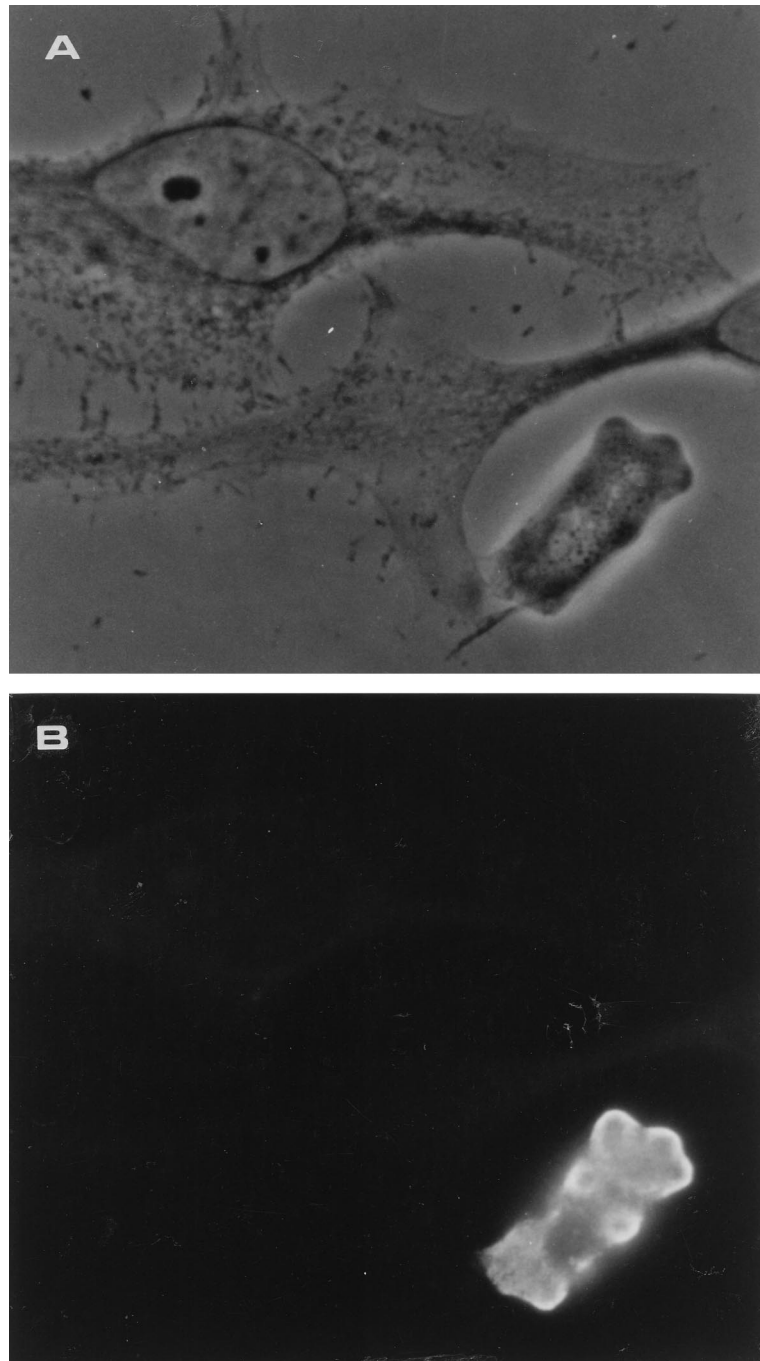
FIG. 3. (A) Phase-contrast micrograph of an amoeboid *T. vaginalis* organism coincubated with HeLa cells. (B) Immunofluorescence pattern of alpha-actinin in the corresponding sample. Cells were fixed and processed for immunofluorescence staining with anti–*T. vaginalis* alpha-actinin antibodies. These images show the lack of cross-reactivity between parasite and host alpha-actinins.

lular regions, a colocalization experiment was performed. Anti–protozoan alpha-actinin and actin antibodies were coincubated with fixed amoeboid parasites adhering on coverslips. Bound anti–alpha-actinin antibodies were identified with fluorescein-conjugated antibodies, while bound antiactin antibodies were identified with rhodamine-conjugated antibodies. The two proteins were observed to colocalize in the same cellular regions of amoeboid parasites. Both actin and alpha-actin were in fact located in pseudopods and adhesion plaques (data not

shown). Preimmune serum and secondary antibodies, used as controls, did not produce any fluorescence of the trichomonad cells.

Expression of trichomonad alpha-actinin mRNA. The changes in intracellular distribution observed for alpha-actinin by immunofluorescence led us to assess whether transformation into the amoeboid morphology involved only the intracellular redistribution of an already existing reservoir of alpha-actinin or whether it was accompanied by enhanced expression
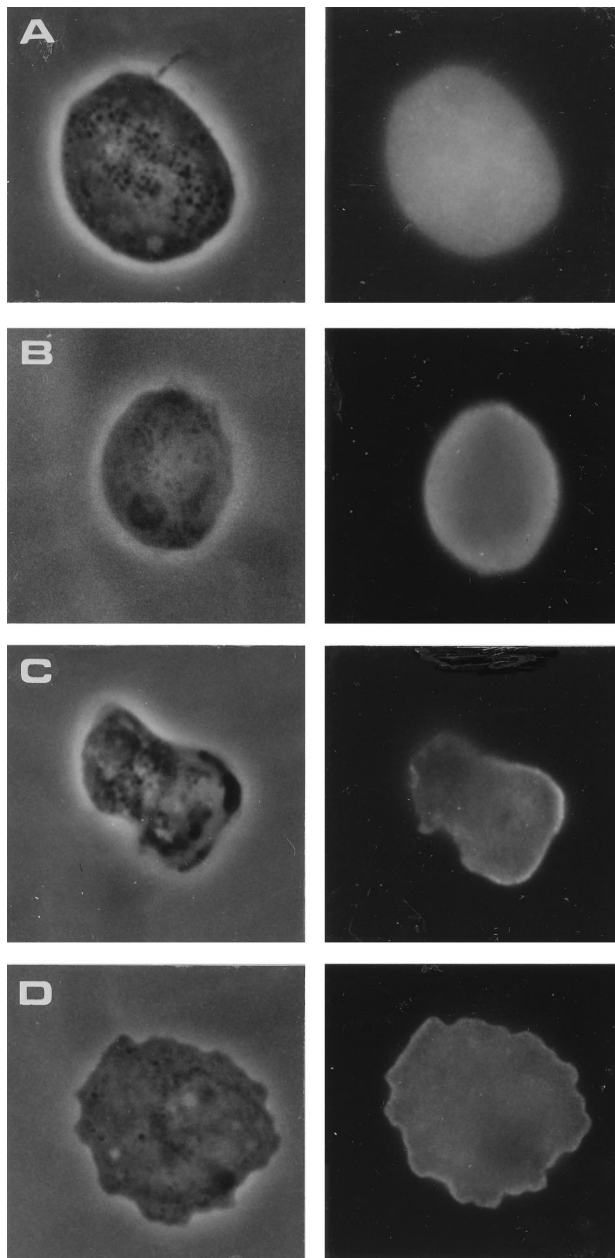
FIG. 4. Distribution of alpha-actinin in different morphological forms of _T. vaginalis_. Living _T. vaginalis_ organisms in suspension and adhering on coverslips were fixed and processed for immunofluorescence staining with anti–_T. vaginalis_ alpha-actinin antibodies. (Right panels) Immunofluorescence patterns of alpha-actinin during different morphological stages of the parasites: A, pear-shaped form; D, fully amoeboid form; B and C, intermediate stages. (Left panel) Phase-contrast micrographs of the corresponding samples. This sequence of images shows the redistribution of alpha-actinin in the periphery of the microorganism following transformation into the amoeboid morphology.

FIG. 5. Representative experiment showing a Northern blot and RT-PCR of total mRNA extracted from pear-shaped (lanes a) and amoeboid (lanes b) _T. vaginalis_ organisms. (Northern blot) Panel 1, hybridization bands obtained with an actin probe; panel 2, hybridization bands obtained with an alpha-actinin probe. (RT-PCR) Panel 3, amplification bands obtained from RNA extracted from pear-shaped and amoeboid parasites with actin primers; panel 4, amplification bands obtained with alpha-actinin primers.

of the alpha-actinin gene. Total RNA was extracted from pear-shaped protozoa grown in suspension and from adherent amoeboid protozoa. Blots of electrophoresed RNA were probed with digoxigenin-labeled probes designed from the _T. vaginalis_ alpha-actinin and actin nucleotide sequences. As shown in Fig. 5, this technique allowed detection of alpha-actinin transcripts only in RNA from amoeboid protozoa (Fig. 5, panel 2, lane b), while actin RNA was detected in equal amounts in both pear-shaped and amoeboid parasites (panel 1, lanes a and b). Ethidium bromide-stained duplicate gels confirmed the presence of equal amounts of total RNA in all lanes. The constant expression of the actin gene was also observed by RT-PCR (Fig. 5, panel 3, lanes a and b), while the differential expression of the alpha-actinin gene was confirmed by the same technique (panel 4, lanes a and b). RT-PCR analysis allowed us to observe that baseline transcription of the alpha-actinin gene occurs in pear-shaped protozoa and to confirm that it undergoes a dramatic increase upon transformation of the protozoan morphology.

DISCUSSION

Important changes in parasite morphology have been demonstrated to occur during _T. vaginalis_ parasitism and colonization of the vaginal epithelium (5). These changes involve transformation of _T. vaginalis_ from an ellipsoidal shape to an amoeboid morphology. The morphological transformation involves signalling and complex intracellular pathways that result in the formation of aggregates of flattened parasites bound to target cells. After transformation and adhesion, target cells are damaged and eventually lysed (16). The ability to undergo morphological changes is presumed to be related to virulence (5). In order to understand the mechanisms which mediate cytopathogenicity, it is important to investigate the cytoskeleton of the microorganism and the mechanisms that regulate the redistribution of its molecular components. That cytoskeletal integrity is important for _T. vaginalis_ cytopathogenicity has been highlighted in the past by Juliano and coworkers (20), who showed that participation of the trichomonad cytoskeleton in interactions with target cells is required, as inferred from the effects of drugs that disrupt cytoskeletal complexes.

In protozoa, several actin-binding proteins participate in movement and morphological changes. In _E. histolytica_, for example, actin-binding proteins play a pivotal role in movement and cellular interactions with the environment (17, 34). It is interesting that _T. vaginalis_ is a flagellated protozoan parasite and that its locomotion is based on flagella; its ability to transform into an amoeboid form is not necessary for movement but is required for cytopathogenicity. Therefore, studying the cytoskeletal organization of this parasite and the mecha-

nisms that regulate the redistribution of cytoskeletal components is of outstanding importance for understanding the mechanisms of pathogenicity.

In this work, we report the nucleotide sequence and molecular characterization of a cDNA coding for *T. vaginalis* alpha-actinin. As far as we know, this is the first alpha-actinin sequence reported for a protozoon. Moreover, *T. vaginalis* diverged relatively early, and detailed knowledge of its cytoskeletal organization and components represents a useful tool in terms of evolutionary studies.

The analysis performed on the sequence obtained from the cloned cDNA revealed homology with alpha-actinins of different species. Homology with other proteins belonging to the actin-binding protein family was also detected; among them, spectrin displayed the highest homology.

The central region of the protein showed less significant homology with alpha-actinins or related proteins. A less conserved central region is found among all actin-binding proteins of the spectrin family; its function is to confer a rod-like structure to this portion of the molecule and is generally the result of shuffling and duplications that occurred during evolution (29).

Analysis of the protein for antigenic determinants revealed that this region contains three high-probability regions of antigenicity. When a *T. vaginalis* total protein extract was injected into rabbits, consistent production of anti–alpha-actinin antibodies was observed, demonstrating the high immunogenicity of the protein. Moreover, data from a study that we performed on patients suffering from trichomoniasis showed that patient sera displayed a strong antibody response to trichomonad alpha-actinin (1a). A test for cross-reactivity was performed on human and several protozoan protein extracts with antibodies directed against the trichomonad protein. An absence of cross-reactivity was observed; human epithelial cells and *G. lamblia*, *E. histolytica*, *A. castellanii*, and *L. major* total protein extracts were not recognized by monospecific anti–*T. vaginalis* alpha-actinin antibodies.

Immunofluorescence analysis demonstrated that *T. vaginalis* alpha-actinin was present throughout the cytoplasm of pear-shaped organisms. Interestingly, when the parasites transformed to the amoeboid morphology, high levels of alpha-actinin were found in the peripheral regions. In particular, highly fluorescent areas could be seen lining pseudopodia and in adhesion plaques. Moreover, we observed by immunofluorescence that actin shows the same peripheral distribution in amoeboid *T. vaginalis*. The peripheral location of actin in the amoeboid protozoan cell has also been reported by Brugerolle et al. (8) using electron microscopy. These findings suggest that alpha-actinin may actively participate in the pathogenic process, playing an important role in mediating the cellular redistribution of actin and therefore in mediating morphological changes.

On these bases, it was interesting to study whether there was only a rearrangement of an already existing intracellular reservoir of the protein or whether there was also enhanced expression of the alpha-actinin gene corresponding to the morphological transformation. Northern blotting and RT-PCR performed on RNA from pear-shaped, resting parasites in liquid cultures and from amoeboid parasites showed that there is an increase in the synthesis of the mRNA coding for the protozoan protein when the microorganism transforms to the amoeboid shape.

Our work started from the observation that the protein was present, together with other proteins, on the membranes of cells lysed by the microorganism. The reasons for the presence of trichomonad alpha-actinin on the target cell surface after lysis remain to be elucidated. However, this is not the first report of intracellular *T. vaginalis* proteins found on the outer environment or on the target cell surface; metabolic enzymes of the parasite have also been reported to bind to target cells (1, 12).

Further studies aimed at identifying the role played by trichomonad alpha-actinin in morphological transformation and parasitism and at clarifying the mechanisms which regulate alpha-actinin expression will hopefully aid in understanding the parasite pathogenic process. Moreover, the cytoskeleton is a good pharmacological target (20, 21); characterization of the *T. vaginalis* cytoskeleton and of its implications in pathogenicity may open the way to designing new pharmacological strategies against this protozoan parasite.

REFERENCES

1. **Addis, M. F., P. Rappelli, P. Cappuccinelli, and P. L. Fiori.** 1997. Extracellular release by *Trichomonas vaginalis* of a NADP$^+$ dependent malic enzyme involved in pathogenicity. Microb. Pathog. **23:**55–61.
1a. **Addis, M. F., et al.** Unpublished data.
2. **Alderete, J. F., and E. Pearlman.** 1984. Pathogenic *Trichomonas vaginalis* cytotoxicity to cell culture monolayers. Br. J. Vener. Dis. **60:**99–105.
3. **Altschul, S. F., T. L. Madden, A. A. Schaffer, J. Zhang, Z. Zhang, W. Miller, and D. J. Lipman.** 1997. Gapped BLAST and PSI-BLAST: a new generation of protein database search programs. Nucleic Acids Res. **25:**3389–3402.
4. **Arroyo, R., J. Engbring, and J. F. Alderete.** 1992. Molecular basis of host epithelial cell recognition by *Trichomonas vaginalis*. Mol. Microbiol. **6:**853–862.
5. **Arroyo, R., A. Gonzàlez-Robles, A. Martìnez-Palomo, and J. F. Alderete.** 1993. Signalling of *Trichomonas vaginalis* for amoeboid transformation and adhesin synthesis follows cytoadherence. Mol. Microbiol. **7:**299–309.
6. **Bradford, M. M.** 1976. A rapid and sensitive method for the quantitation of microgram quantities of protein utilizing the principle of protein-dye binding. Anal. Biochem. **72:**248–254.
7. **Bricheux, G., and G. Brugerolle.** 1997. Molecular cloning of actin genes in *Trichomonas vaginalis* and phylogeny inferred from actin sequences. FEMS Microbiol. Lett. **153:**205–213.
8. **Brugerolle, G., G. Bricheux, and G. Coffe.** 1996. Actin cytoskeleton demonstration in *Trichomonas vaginalis* and in other trichomonads. Biol. Cell **88:**29–36.
9. **Chomczynski, P., and N. Sacchi.** 1987. Single-step method of RNA isolation by acid guanidinium thiocyanate-phenol-chloroform extraction. Anal. Biochem. **162:**156–159.
10. **Diamond, L. S.** 1957. The establishment of various trichomonads of animals and man in axenic cultures. J. Parasitol. **43:**488–490.
11. **Diamond, L. S.** 1961. Axenic cultivation of *Entamoeba histolytica*. Science **134:**336–337.
12. **Engbring, J. A., J. L. O'Brien, and J. F. Alderete.** 1996. Trichomonas vaginalis adhesin proteins display molecular mimicry to metabolic enzymes. Adv. Exp. Med. Biol. **408:**207–223.
13. **Fiori, P. L., P. Rappelli, M. F. Addis, F. Mannu, and P. Cappuccinelli.** 1997. Contact-dependent disruption of the host cell membrane skeleton induced by *Trichomonas vaginalis*. Infect. Immun. **65:**5142–5148.
14. **Fiori, P. L., P. Rappelli, M. F. Addis, A. Sechi, and P. Cappuccinelli.** 1996. *Trichomonas vaginalis* haemolysis: pH regulates a contact-independent mechanism based on pore-forming proteins. Microb. Pathog. **20:**109–118.
15. **Fiori, P. L., P. Rappelli, A. M. Rocchigiani, and P. Cappuccinelli.** 1993. *Trichomonas vaginalis* haemolysis: evidence of functional pore formation on red cell membranes. FEMS Microbiol. Lett. **109:**13–18.
16. **Gonzales-Robles, A., A. Lazaro-Haller, M. Espinosa-Castellano, F. Anaya-Velazques, and A. Martinez-Palomo.** 1995. *Trichomonas vaginalis*: ultrastructural basis of the cytopathic effect. J. Eukaryot. Microbiol. **42:**641–651.
17. **Guillen, N.** 1996. Role of signalling and cytoskeletal rearrangements in the pathogenesis of *Entamoeba histolytica*. Trends Microbiol. **4:**191–196.
18. **Gupta, P. K., and J. K. Frost.** 1989. Cytopathology and histopathology of female genital tract in *Trichomonas vaginalis* infection, p. 274–290. *In* B. M. Honigberg (ed.), Trichomonads parasitic in humans. Springer-Verlag, New York, N.Y.
19. **Honigberg, B. M.** 1978. Trichomonads of importance in human medicine, p. 275. *In* J. P. Kreier (ed.), Parasitic protozoa, vol. II. Academic Press, Inc., New York, N.Y.
20. **Juliano, C., G. Monaco, P. Bandiera, G. Tedde, and P. Cappuccinelli.** 1987. Action of anticytoskeletal compounds on in vitro cytopathic effect, phago-

cytosis, and adhesiveness of *Trichomonas vaginalis*. Genitourin. Med. **63:** 256–263.

21. **Juliano, C., G. Monaco, S. Rubino, and P. Cappuccinelli.** 1986. Inhibition of *Trichomonas vaginalis* replication by the microtubule stabilizer taxol. J. Protozool. **33:**255–260.

22. **Juliano, C., S. Rubino, D. Zicconi, and P. Cappuccinelli.** 1986. An immunofluorescence study of the microtubule organisation in *Trichomonas vaginalis* using antitubulin antibodies. J. Protozool. **33:**56–59.

23. **Keeling, J. K., A. L. Doherty-Kirby, E. M. Teh, and W. Ford Doolittle.** 1996. Linked genes for calmodulin and E2 ubiquitin-conjugating enzyme in *Trichomonas vaginalis*. J. Eukaryot. Microbiol. **43:**468–474.

24. **Krieger, J. N.** 1981. Urologic aspects of trichomoniasis. Investig. Urol. **18:** 411–417.

25. **Krieger, J. N., J. I. Ravdin, and M. F. Rein.** 1985. Contact-dependent cytopathogenic mechanism of *Trichomonas vaginalis*. Infect. Immun. **50:**778–786.

26. **Laemmli, U. K.** 1970. Cleavage of structural proteins during the assembly of the head of bacteriophage T4. Nature **227:**680–685.

27. **Laga, M., A. Manoka, M. Kivuvu, B. Malele, M. Tuliza, N. Nzila, J. Goeman, F. Behets, V. Batter, M. Alary, W. L. Heyward, R. W. Ryder, and P. Piot.** 1993. Non-ulcerative sexually transmitted diseases as risk factors for HIV-1 transmission in women: results from a cohort study. AIDS **7:**95–102.

28. **Moskowitz, M. O., and B. C. Mellinger.** 1992. Sexually transmitted diseases and their relation to male infertility. Urol. Clin. North Am. **19:**35–45.

29. **Pascual, J., J. Castresana, and M. Saraste.** 1997. Evolution of the spectrin repeat. Bioessays **9:**811–817.

30. **Pearson, W. R., and D. J. Lipman.** 1988. Improved tools for biological sequence comparison. Proc. Natl. Acad. Sci. USA **85:**2444–2448.

31. **Rappelli, P., A. M. Rocchigiani, G. Erre, M. M. Colombo, P. Cappuccinelli, and P. L. Fiori.** 1995. Sequence of cDNA coding for a 65 kD adhesive protein for the specific detection of *Trichomonas vaginalis* by PCR. FEMS Microbiol. Lett. **129:**21–26.

32. **Sambrook, J., E. F. Fritsch, and T. Maniatis.** 1989. Molecular cloning: a laboratory manual, 2nd ed. Cold Spring Harbor Laboratory Press, Cold Spring Harbor, N.Y.

33. **Tufty, R. M., and R. H. Kretsinger.** 1975. Troponin and parvalbumin calcium binding regions predicted in myosin light chain and T4 lysozyme. Science **187:**167–169.

34. **Vargas, M., P. Sansonetti, and N. Guillen.** 1996. Identification and cellular localisation of the actin-binding protein ABP-120 from *Entamoeba histolytica*. Mol. Microbiol. **22:**849–857.

35. **Wasserheit, J. N.** 1992. Interrelationship between human immunodeficiency virus infection and other sexually transmitted diseases. Sex. Transm. Dis. **19:**61–77.

36. **Zanetti, S., P. L. Fiori, A. Pinna, S. Usai, F. Carta, and F. Fadda.** 1995. Susceptibility of *Acanthamoeba castellanii* to contact lens disinfecting solutions. Antimicrob. Agents Chemother. **39:**1596–1598.

37. **Zhang, Z. F., and C. B. Begg.** 1994. Is *Trichomonas vaginalis* a cause of cervical neoplasia? Results from a combined analysis of 24 studies. Int. J. Epidemiol. **23:**682–690.

Editor: P. J. Sansonetti